The role of *F-cadherin* in localizing cells during neural tube formation in *Xenopus* embryos

Amy Espeseth[1], George Marnellos[2,3] and Chris Kintner[1],*

[1]Molecular Neurobiology Laboratory, and [2]Sloan Center for Theoretical Neurobiology, The Salk Institute for Biological Studies, PO Box 85800, San Diego, 92186, USA
[3]Section of Neurobiology, Yale University, New Haven, CT, USA
*Author for correspondence (e-mail: Kintner@sc2.salk.edu)

SUMMARY

The cell adhesion molecule F-cadherin is expressed in *Xenopus* embryos at boundaries that subdivide the neural tube into different regions, including one, the sulcus limitans, which partitions the caudal neural tube into a dorsal and ventral half (alar and basal plate, respectively). Here we examine the role of F-cadherin in positioning cells along the caudal neuraxis during neurulation. First, we show that ectopic expression of *F-cadherin* restricts passive cell mixing within the ectodermal epithelium. Second, we show that *F-cadherin* is first expressed at the sulcus limitans prior to the extensive cell movements that accompany neural tube formation, suggesting that it might serve to position cells at the sulcus limitans by counteracting their tendency to disperse during neurulation. We test this idea using an assay that measures changes in cell movements during neurulation in response to differential cell adhesion. Using this assay, we show that cells expressing *F-cadherin* localize preferentially to the sulcus limitans, but still disperse when located away from the sulcus limitans. In addition, inhibiting cadherin function prevents cells from localizing precisely at the sulcus limitans. These results indicate that positioning of cells at the sulcus limitans is mediated in part by the differential expression of *F-cadherin*.

Key words: F-cadherin, Neural tube, Sulcus limitans, Cell movement, Cell adhesion, *Xenopus*

INTRODUCTION

During the development of the vertebrate central nervous system (CNS), the neuroepithelium of the neural tube is divided into distinct regions with different developmental fates. This process begins during neurulation when the CNS first forms as a neural tube with distinct dorsoventral (D-V) and anteroposterior (A-P) axes. One likely outcome of neural patterning is to endow neural cells with the ability to precisely position along the neuraxis, even during periods of tissue morphogenesis when extensive cell movements occur. However, the mechanisms by which cells are localized to particular regions within the developing CNS remain poorly understood.

One mechanism proposed to determine cell position within the neural tube is differential cell adhesion as mediated by members of the cadherin family. This family of cell adhesion molecules consists of integral membrane proteins with conserved domains that allow for protein-protein interactions on both sides of the plasma membrane. The cadherin extracellular domain binds homotypically, thus promoting adhesion between adjacent cells expressing the same cadherin type. Cell adhesion, moreover, requires interactions between the conserved intracellular domain and the cytoplasmic catenin proteins which link the cadherins to the actin-based cytoskeleton (Ozawa et al., 1989). Both interactions allow the cadherins to serve as the transmembrane linkage in a specialized cell-cell contact site, termed the adherens junction (Geiger and Ayalon, 1992). By linking the actin cytoskeleton of adjacent cells, the cadherins are particularly well positioned to regulate cell movements that underlie morphogenesis. In addition, the ability of the cadherins to mediate cell sorting in vitro suggests that the differential expression of cadherins could mediate the preferential association of cells, allowing cells to position themselves within the developing CNS (Takeichi, 1991, 1995).

A number of cadherins have been identified that are expressed in developing neural tissue. One of these, *N-cadherin*, is expressed by a majority of the neuroepithelial cells of the developing neural tube (Hatta et al., 1987). Disruption of the *N-cadherin* gene by homologous recombination results in homozygous mutant mice with severe neural tube defects, suggesting a role for N-cadherin in the formation of neural tissue (Hynes, 1996). Other members of the cadherin family have been identified which are expressed in subregions of the neural tube, and thus could be involved in mediating differential adhesion among neuroepithelial cells. For example, *E-cadherin*, which is expressed extensively outside the nervous system, displays a restricted pattern of expression in developing brain (Redies and Takeichi, 1993; Shimamura and

Takeichi, 1992). *R-cadherin* is also expressed in restricted subdomains of the developing brain that include neuromere boundaries and a subset of developing nuclei (Ganzler and Redies, 1995; Matsunami and Takeichi, 1995; Redies et al., 1993). In addition, several of the type II cadherins and protocadherins are also expressed in subregions of neural tissue (Nakagawa and Takeichi, 1995; Redies and Takeichi, 1996; Sano et al., 1993; Suzuki et al., 1991). Thus, the differential expression of cadherin family members during neural development lends further support to the model that these molecules form subdomains within neural tissue.

We have previously described F-cadherin as a type II cadherin that is expressed by a subpopulation of neuroepithelial cells in the developing neural tube of *Xenopus* embryos. *F-cadherin*-expressing cells often lie at boundaries that subdivide the neural tube into different regions along the neuraxis (Espeseth et al., 1995). One of these boundaries, termed the sulcus limitans, divides the caudal neural tube into a dorsal half, involved in sensory function (the alar plate), and a ventral half involved in motor function (the basal plate). *F-cadherin* expression at the sulcus limitans first appears at the open neural plate stage (see Fig. 2) when the neural anlage is initially patterned. During neurulation, the neural anlage undergoes a morphogenetic process, called convergent-extension (C-E), during which cells tend to disperse along the D-V neuraxis. Nonetheless, the stripe of cells expressing *F-cadherin* remains at the sulcus limitans, and even sharpens in width during neurulation (Espeseth et al., 1995). Thus, if F-cadherin prevents cells from dispersing during C-E, then this might explain how cells that express *F-cadherin* localize to the sulcus limitans during neural tube formation.

Here we test the role of F-cadherin in determining cell position along the D-V axis of the caudal neural tube. We first show that ectopic expression of *F-cadherin* restricts passive cell mixing within the ectoderm, creating a boundary between *F-cadherin* and non-*F-cadherin*-expressing cells. We then employ a transplantation assay to determine whether ectopic expression of *F-cadherin* can influence cell position during neural tube formation. Using this assay, we show that cells-expressing *F-cadherin* localize preferentially to the sulcus limitans, but still disperse when located away from the sulcus limitans. We also show that cells expressing an inhibitor of F-cadherin fail to localize precisely at the sulcus limitans. Finally, we show that cells disperse even further than normal along the D-V axis of the neural tube when they express a pan-inhibitor of cadherin function. These observations, supplemented with a computer model of cell dispersion during neurulation, suggest that cells require F-cadherin, along with other factors, to localize to the sulcus limitans during neural tube formation.

MATERIALS AND METHODS

In vitro RNA synthesis

A template for the in vitro synthesis of *F-cadherin* RNA was constructed by inserting the *F-cadherin* cDNA into the CS2 vector (Turner and Weintraub, 1994), and linearizing the vector DNA with *Not*I. A myc-tagged version of *F-cadherin* was constructed by fusing in-frame, 6 copies of the myc-epitope sequence at the carboxyl terminus (Turner and Weintraub, 1994). The CBR-MT construct has been described previously (Riehl et al., 1996). The cDNA encoding ΔF-cadherin was constructed by introducing the 6 copies of the myc

epitope into the F-cadherin sequence 8 amino acids after the transmembrane domain, followed by a stop codon. The myc-tagged versions of F-cadherin, ΔF-cadherin and CBR were used to show that protein expression from injected RNAs persisted out to neurulae stages. Capped RNAs encoding F-cadherin and ΔF-cadherin were synthesized in vitro using standard techniques (Kintner, 1988).

Ectoderm mixing assay

In vitro transcribed mRNAs encoding β-galactosidase or myc-tagged forms of F-cadherin and ΔF-cadherin (0.25-1.0 ng/embryo) were injected into single blastomeres of 8-16 cell embryos. After embryos had completed gastrulation (st. 12.5), they were fixed in MEMFA, and either stained in whole-mount for β-galactosidase expression in 0.15% X-gal in 0.1 M ferricyanide, 0.1 M ferrocyanide, and 0.1 M sodiun phosphate, pH 6.3, or for the myc-epitope using a monoclonal antibody (Evan et al., 1985) and HRP immunohistochemistry. After staining, embryos with a patch of labeled cells within the ventral ectoderm were selected and mounted under a coverslip. Using camera-lucida, the edge of patches of labeled cells was drawn, as well as any labeled cells lying outside of the patch, or unlabeled cells lying within the patch of labeled cells. The number of isolated cells in a measured area was counted for at least five embryos injected with a given RNA, and then expressed as the average number of isolated cells per square millimeter of epithelium.

Transplantation assay and bin analysis

Synthetic *nLacZ* RNA (0.4 ng/embryo) or a mixture of *nLacZ* and experimental RNA (1.0 ng/embryo) was injected, in a volume of 10 nl, into the animal pole of all four blastomeres of donor embryos at the four cell stage (Coffman et al., 1993). Tissue (15-30 cells) was isolated from the ectoderm of donor embryos at stage 10, and placed into host embryos shortly after the formation of the blastopore lip (st. 10.5). In the case of alar plate transplants, donor cells were placed between 45 and 90 degrees from the center of the blastopore lip of the host, while for basal plate transplants, the donor cells were placed between 20-45 degrees. After host embryos had reached neurulae stages, they were fixed in MEMFA, reacted for β-galactosidase expression in 0.15% salmon-gal (Molecular Probes) or X-gal as described above and then double stained by whole-mount in situ hybridization (Harland, 1991) for expression of *F-cadherin* RNA (Espeseth et al., 1995). After postfixing in MEMFA, stained embryos were embedded in Paraplast, sectioned at 10 μm on a rotary microtome, and mounted on glass slides in Permount. Using camera lucida, a grid subdividing the neural tube was used to assign donor nuclei into each bin along the dorsal ventral axis (see Fig. 4). Embryos with 20-220 cells were included in the subsequent analysis of cell distributions. The distribution of transplanted cells was plotted for each embryo by assigning the cells to bins as described in Fig. 4. Average distributions were obtained by first assigning each transplant a peak location corresponding to the bin containing the largest number of transplanted cells, and then averaging the data from transplants with the same peak location.

In order to compare the spread of transplant distributions for the various kinds of transplants, we also looked at the full width at half maximum (FWHM) of transplant distributions in individual embryos; this was measured in number of bins and the values ranged between 1 and 6. We calculated the FWHM means and standard deviations for two groups of embryos for each kind of transplant: one group consisted of the embryos that had at least 30% of transplant cells at the sulcus limitans, the 'sulcus limitans group', and the other contained the rest of the embryos, the 'away from the sulcus limitans group'. We carried out pairwise comparisons of these means for different kinds of transplants and tested the statistical significance of their differences using a *t*-test. This analysis was done for embryos with dorsal transplants; there were not enough embryos with ventral transplants to carry out meaningful statistical comparisons. Embryos with bimodal transplant cell distributions were excluded from the FWHM analysis. The results of the FWHM analysis are presented in Table 3.

Computer simulations

Computer simulations were used to model the movements of transplanted cells in the neural plate during neurulation. The tissue is modeled as a 2-dimensional rectangular grid at the vertices of which the cells are placed. At the start of a simulation the tissue has 18(A-P)×56(D-V) cells, each placed on a single vertex; a 6×6 patch of those cells (corresponding to a transplant) is labeled differently from the rest (see Fig. 10 B,C); each cell has an adhesion value indicating the adhesion strength expressed by the cell (we assume a default adhesion for all cells).

In the model, elongation of the tissue proceeds in a repeating succession of two steps, a step of random cell rearrangement on the grid and a step of cells moving subject to adhesive forces and opposing diffusion-like forces that tend to spread cells uniformly on the grid. These steps are intended to model cell intercalation. During the *rearrangement* step, cells move one position up or down and left or right; cells on the left and right borders of the tissue move only to the right or left respectively; this is done in such a way that after a rearrangement step there is one column of cells less than before. Rows are added to the top and bottom of the grid, so that the total number of grid points stays about the same. Even though at the beginning there is exactly one cell at each grid point, during the run more than one cells can be at the same grid position and of course a grid position may be unoccupied (see Fig. 10A). It should be emphasized at this point that the model described here is not a model of how C-E itself occurs, since convergence is imposed during the rearrangement step (and extension follows to some degree from that), but a model of how, given the shape changes of a tissue undergoing C-E, cells, moving stochastically and interacting adhesively with each other, disperse on the elongating tissue.

During the *diffusion-adhesion* step, one random grid position **r** on the tissue is selected at a time; for each cell $cell_i$ at position **r** the adhesion A experienced by the cell is calculated, by summing the adhesion values of the cells in the neighborhood, as described in the following equation

$$A(\mathbf{r},cell_i) = \sum_{j \in N} \lambda_j f(v_i, v_j) \,,$$

where N is the set of cells in the neighborhood, i.e. the set of all cells at position **r** and the surrounding 8 grid positions (or 5 positions if **r** is at the border or 3 if it is one of the corners); the v's are adhesion types of individual cells, f a function taking different values for different kinds of adhesive interactions; the λ_j's are weights of the terms in the sum (in the runs described here they are all equal to 1.0).

More specifically, f takes a default value 1.0 for all kinds for cell-cell contacts, which would correspond to non-specific adhesive interactions and friction. For border-cell/border-cell interactions f takes the value 4.0 (= 3.0 plus the default value). For patch-cell/patch-cell interactions, depending on the condition being tested, f takes either the value 1.0 (= just the default value), which corresponds to the 'patch non-adhesive to itself' condition, or the value 2.0 (= 1.0 plus the default value), which corresponds to the 'patch adhesive to itself' condition. For patch-cell/border-cell interactions, again depending on the condition being tested, f takes either the value 1.0 (= just the default value), which corresponds to the 'patch non-adhesive to border' condition, or the value 4.0 (= 3.0 plus the default value), which corresponds to the 'patch adhesive to border' condition.

We next compute an estimate of how 'energetically' favored a cell move is, either from position **r** to the surround (i.e. the grid points around position **r**) or from the surround to **r**. We call this estimate the *Energy* of the move of cell $cell_i$, from position $\mathbf{r}_{start}$ to position $\mathbf{r}_{end}$ and it essentially compares the difference in cell density between the start and end positions with the difference in adhesion the cell would experience in these two positions: an energetically favored move would tend to move a cell from a position of higher cell density to

one of lower cell density and from a position of lower adhesion to one of higher adhesion. We calculate the *Energy* of a move as follows:

$$Energy(cell_i, \mathbf{r}_{start}, \mathbf{r}_{end}) = w_d\, bias\,[D(\mathbf{r}_{end}) - D(\mathbf{r}_{start})] - $$
$$w_a[A(\mathbf{r}_{end},cell_i) - A(\mathbf{r}_{start},cell_i)]$$

where $D(\mathbf{r})$ is the number of cells at position **r** (i.e. cell density at **r**); $A(\mathbf{r},cell_i)$ is the adhesion $cell_i$ would experience at position **r** (as given in the equation above); w_d and w_a are weights that determine the relative contribution of the cell density and adhesion differences (in the runs presented here these had the values w_d=1.0 and w_a=0.0002). The lower (more negative) *Energy* is, the more energetically favored the move is.

The *bias* factor in the *Energy* expression above is meant to simulate 'convective' flows of large numbers of cells in the neural plate that would tend to bias local movements of individual cells. It may take values from 0.0 to 1.0 and tends to be higher for moves towards the midline in the horizontal D-V direction and for outward moves in the vertical A-P direction and; as long as it favors such moves, the precise detail of how it is computed do not seem to matter in our simulations: in our runs the bias factor is a non-linear sum

$$bias = S(DVbias + APbias)$$

of a D-V (horizontal) component, *DVbias*, and an A-P (vertical) component *APbias*; *DVbias* is proportional to the distance of the end position from the closest (either left or right) border and is positive if the move is towards the midline (and negative otherwise); similarly, *APbias* is proportional to the distance of the end position from the A-P midline and is positive if the move is outward either towards the anterior or posterior (and negative otherwise). Function S takes the value *DVbias* + *APbias*, if this sum is between 0.0 and 1.0; 0.0 if this sum is negative; and 1.0, if this sum is greater than 1.0. Although it might appear that the bias factor could counteract cell mixing and lead to very narrow distributions of patch cells, this is not the case; on the contrary, patch cell distributions can be very broad (depending on other parameters of the model). However, if the bias factor is not included, then cells tend to accumulate at the borders as the tissue elongates.

When the energies of all possible cell moves from position **r** to the surround or vice versa have been computed, the move with the lowest negative energy is chosen, i.e. we look for

$$\min_{i \in N} Energy(cell_i, \mathbf{r}_{i,\,start}, \mathbf{r}_{i,\,end})\,,$$

and also minimizing for all possible pairs of start and end positions i.e. with $\mathbf{r}_{i,end} \in Surround$ if $\mathbf{r}_{i,start}$ = **r**, or $\mathbf{r}_{i,end}$ = **r** if $\mathbf{r}_{i,start} \in Surround$, where N is the set of all cells in the neighborhood of position **r** (as in the first equation above) and *Surround* is the set of grid positions surrounding **r**.

During 25% of the time, or when no moves have negative energy, a move is selected at random from all the possible moves. This process is repeated about 100 times during each diffusion-adhesion step at randomly chosen grid positions which uniformly cover the whole extent of the tissue.

After several rounds of such rearrangement and diffusion-adhesion steps the tissue has elongated (as the neural tube does) and shrunk in width to a final grid with 16 points in the D-V direction (see Fig. 10B,C); we run one hundred simulations under each condition and gather statistics about the final distribution of patch cells on the grid (see Fig. 10D). Such information can be 'collapsed' to one dimension to produce histograms of the distributions of patch cells in the D-V direction, as in Fig. 6 of the Results.

RESULTS

F-cadherin inhibits cell mixing in ventral ectoderm

The predicted structural features of F-cadherin suggest that it mediates homotypic adhesion, as reported for other members of

the type II cadherin family (Nakagawa and Takeichi, 1995; Suzuki et al., 1991). If so, one would predict that embryonic cells that differentially express *F-cadherin* would stick together and not mix with cells not expressing *F-cadherin*. As a first test of this prediction, we ectopically expressed *F-cadherin* in the ectoderm of early *Xenopus* embryos. RNA encoding a myc-tagged form of F-cadherin was injected into one animal blastomere at the 8-16 cell stage, thus restricting the expression of the injected RNA to a subpopulation of ectodermal cells. The embryos were allowed to develop through gastrulation which normally causes passive cell mixing among ectodermal cells (Detrick et al., 1990). At stage 12.5, embryos were fixed and stained for the expression of the epitope-tagged F-cadherin in order to determine the degree of mixing between F-cadherin-expressing cells and non-expressing cells (Fig. 1). The results show that cells expressing *F-cadherin* mixed much less with non-expressing cells than did cells in control embryos injected with *lacZ* alone (Fig. 1D). In addition, staining with the myc antibody shows that F-cadherin is concentrated at the site of contact between *F-cadherin*-expressing cells, suggesting that F-cadherin mediates adhesion by homotypic binding (Fig. 1B). Thus, these results show that differential expression of *F-cadherin* can suppress cell mixing within the embryonic ectoderm.

We constructed an antimorphic form of F-cadherin, called ΔF-cadherin, which lacks the intracellular domain. Similarly deleted forms of other members of the cadherin family have been shown to be markedly deficient in adhesion in cell mixing assays, and even to act as dominant-negative mutants, presumably by binding extracellularly to like-cadherins, without interacting with cytoplasmic components required for adhesion (Kuhl et al., 1996; Lee and Gumbiner, 1995; Levine et al., 1994). As predicted, ΔF-cadherin did not significantly affect cell mixing when ectopically expressed in the ectoderm, suggesting that the F-cadherin cytoplasmic domain is required for its function (Fig. 1 C,D). To ask whether ΔF-cadherin can act as a dominant-negative mutant, we mixed *F-cadherin* and *ΔF-cadherin* mRNA in different ratios, and introduced these mixtures into the ectoderm. The results show that when F-cadherin and ΔF-cadherin are expressed together, ΔF-cadherin inhibits the adhesive activity of F-cadherin, suggesting that ΔF-cadherin can act as a dominant negative inhibitor of F-cadherin (Fig. 1D).

Ectopic expression of *F-cadherin* disrupts C-E

Expression of *F-cadherin* is first detected at stage 12.5 (open neural plate stage) in two lateral domains of the neural plate that correspond in position to the prospective sulcus limitans (Espeseth et al., 1995). At this stage, the width of the caudal neural plate along its prospective D-V axis is two-fold greater than its length along the A-P axis. The neural anlage then undergoes a remarkable transformation in shape by narrowing along the D-V axis and lengthening along the A-P axis, resulting in a neural tube which is ten-fold longer along the A-P axis, than along the D-V axis. This change in shape, called convergent-extension (C-E), is brought about in part by active cell intercalation, resulting in extensive cell mixing along both the D-V and A-P neuraxis (Keller et al., 1992). During neural tube formation, *F-cadherin* expression is detected on a coherent stripe of cells that lie at the future sulcus limitans (Fig. 2). Thus, these observations suggested that differential expression of *F-cadherin* might contribute to the localization of cells to the sulcus limitans during a period of active cell movement.

As a first test of whether differential expression of *F-cadherin* might affect cell movements during C-E, we ectopically expressed *F-cadherin* on one side of the embryo by RNA injections at the two-cell stage (Fig. 3). Embryos were left to develop until late neural plate stages, and the extent of C-E was then measured by staining the embryos with a probe for *N-tubulin*, which marks the formation of primary neurons.
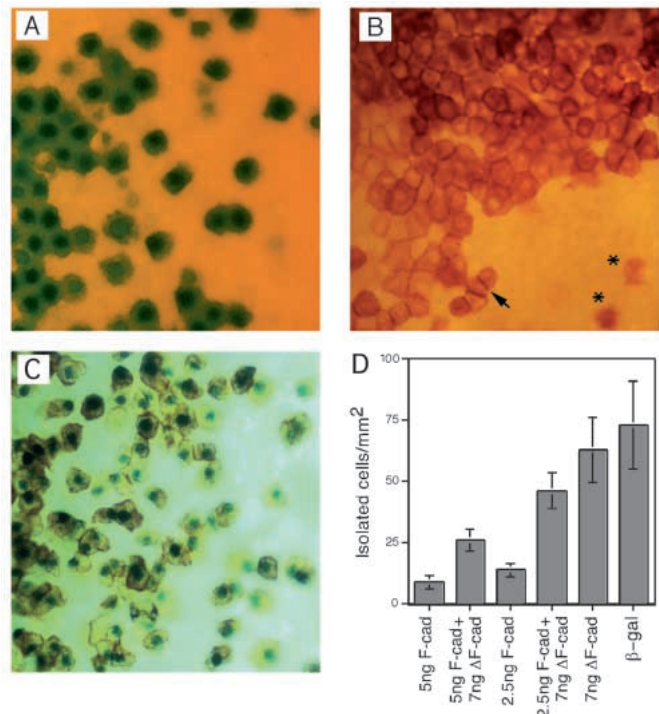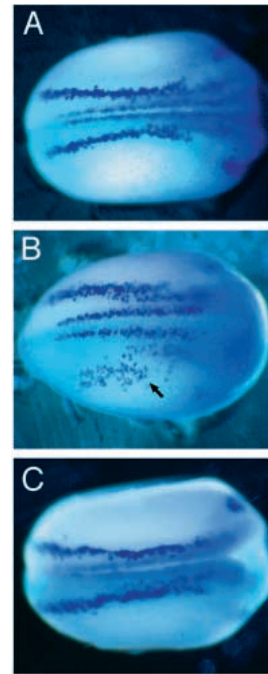

Fig. 1. Ectoderm mixing assay. (A) One blastomere of a 16-32 cell stage embryo was injected with *nLacZ* RNA. At stage 12, the embryo was fixed and processed for X-gal staining. Shown are X-gal-stained cells derived from the injected blastomere within the ventral ectoderm. Note that these cells have intermingled with descendants of neighboring blastomeres. (B) One blastomere of a 16-32 cell stage embryos was injected with RNA encoding F-cadherin. At stage 12, the embryo was fixed and stained for the myc epitope. Shown are myc antibody-stained cells derived from the injected blastomere within the ventral ectoderm. Note that these cells have not intermingled to the same extent as in A. Asterisks indicate cells in the deep layer of ectoderm where mixing is not suppressed by F-cadherin expression. Arrowheads indicate the enrichment of expressed protein at sites of cell-cell contact. (C) Same analysis as in B except that the embryos were injected with RNA encoding ΔF-cadherin. Note that these cells mix as well as control cells. (D) *F-cadherin* and *ΔF-cadherin* RNAs were mixed at different ratios and injected into a blastomere of a 16-32 cell stage embryo. At stage 12, embryos were fixed and stained for the myc-epitope. The number of isolated cells per unit area at the edge of a patch of labeled cells was analyzed for 6-12 embryos, and their mean and standard error calculated. Note that cell mixing is significantly reduced with both high (5 ng) and low (2.5 ng) concentrations of *F-cadherin* RNA relative to β-gal controls ($P<0.001$ and $P<0.01$, respectively, using one-tailed *t*-tests). Co-injection of *ΔF-cadherin* RNA with *F-cadherin* RNA inhibits the effects of *F-cadherin* on cell mixing: note that cell mixing is significantly increased when *ΔF-cadherin* (7 ng) is included with *F-cadherin*, relative to when 5 ng or 2.5 ng of *F-cadherin* RNA is injected alone ($P<0.005$ in both cases, using a one-tailed *t*-test). Embryos injected with 7 ng ΔF-cadherin and β-gal controls were not statistically different for $P<0.10$ (using a *t*-test).
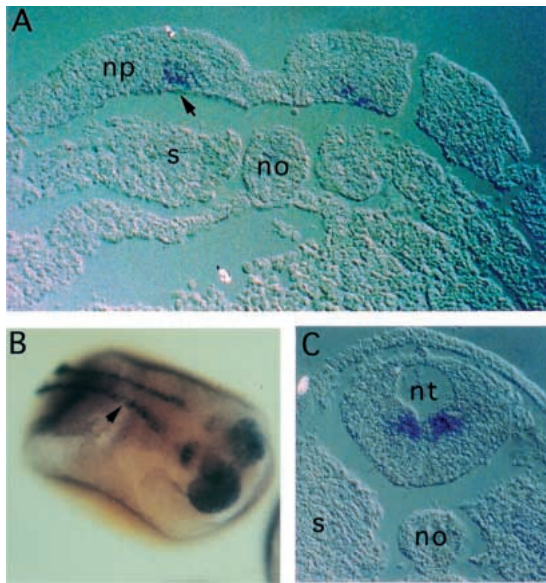
Fig. 2. Expression of *F-cadherin* RNA during neural tube formation in *Xenopus* embryos. Embryos at stage 16 (neural plate stage) and stage 22 (early neurulae) were stained for the expression of *F-cadherin* RNA using whole mount in situ hybridization. (A,B) Stage 16 embryo stained for *F-cadherin* expression showing the stripe of *F-cadherin*-expressing cells within the caudal neural anlage, either in whole mount (B, arrow) or in a transverse section through the neural plate (A, arrow). Note that *F-cadherin*-expressing cells are already localized to the prospective sulcus limitans, based on their position within the neural plate (np) along the mediolateral axis. (C) After neural tube formation, *F-cadherin* is expressed in cells localized to the sulcus limitans, which divide the neural tube (nt) along the D-V axis into the basal and alar plate. Note in panel C that the cells with *F-cadherin* staining lie adjacent to the ventricle, but that this staining is probably confined to the cell body. Thus, it is likely that the cells expressing *F-cadherin* RNA are neuroepithelial, or radial glial cells, that span the neural tube from the lumen to the pial surface.

Fig. 3. Effects of F-cadherin and ΔF-cadherin on convergent-extension. One blastomere at the two-cell stage was injected twice with (A) *nLacZ* RNA, (B) a mixture of *nLacZ* and *F-cadherin* RNA or (C) a mixture of *nLacZ* and Δ*F-cadherin* RNA. At late neural plate stages the embryos were fixed and stained with X-gal to reveal the injected side (arrow in panel B), and for for *N-tubulin* expression using whole mount in situ hybridization to reveal the position of the primary neurons (Chitnis et al., 1995). Note that injection of *F-cadherin*, but not *nLacZ* or Δ*F-cadherin* RNA significantly alters C-E as revealed by the effects on the position of primary neurons. The embryo in panel B is slightly younger in age than those shown in Panels A and C.

Primary neurons first form at the open neural plate, in three longitudinal domains on both sides of the midline (Chitnis et al 1995). During neurulation, these domains undergo a change in shape and position that mirrors the overall change in shape of the neural plate during C-E. In embryos ectopically expressing *F-cadherin*, the stripes of primary neurons form properly but fail to converge and extend normally on the injected side (Fig. 3). This result indicates that ectopic expression of *F-cadherin* perturbs C-E, in line with previous observations showing that

perturbation in cadherin function can alter C-E in the mesoderm (Kuhl et al 1996; Lee and Gumbiner, 1995). In addition, we ectopically expressed Δ*F-cadherin* on one side of *Xenopus* embryos by RNA injection and assessed the effects of this on C-E by staining for the formation of primary neurons (Fig. 3; Table 1). In contrast to *F-cadherin,* ectopic expression of Δ*F-cadherin* did not appear to have a dramatic affect on C-E as measured by the pattern of primary neurons, suggesting as above that the cytoplasmic domain is required for F-cadherin function (Figs 1, 3; Table 1). In addition, examination of the Δ*F-cadherin*-expressing embryos revealed none of the lesions

Table 1. Effects of *F-cadherin* on the distribution of primary neurons

Injected RNA (# embryos)	Lateral stripelength (mm)			Lateral stripe width (mm)		
	Injected side	Control side	P(T<=*t*)	Injected side	Control side	P(T<=*t*)
F-cadherin (*n*=17)	0.68±0.05	0.87±0.03	2.7×10^{-5}	0.40±0.04	0.24±0.02	6.7×10^{-5}
Δ*F-cadherin* (*n*=11)	1.20±0.04	1.17±0.03	0.192	0.21±0.01	0.16±0.01	0.005
nlacZ (*n*=22)	0.91±0.04	0.89±0.04	0.25	0.24±0.01	0.25±0.02	0.30

Embryos were injected with the indicated RNAs and processed for the *N-tubulin* staining as described in the legend to Fig. 3. Both the width and the length of the lateral stripe of primary neurons was measured under a dissecting microscope using a micrometer. Note that *F-cadherin* causes both an increase in width and a decrease in length of the lateral domain of primary neurons, consistent with an inhibition of C-E. In contrast, Δ*F-cadherin* produces only a small effect on width but not length of the primary neurons.

Table 2. Distribution of transplants along the D-V neuraxis

Transplant	Bin*	No. transplants with peak†	%‡
β-gal (n=69)	RP	4	6
	1	11	16
	2	9	13
	3	5	7
	SL	17	**24.5**
	5	8	11.5
	6	5	7
	7	8	11.5
	FP	2	2
F-cadherin (n=40)	RP	2	5
	1	6	15
	2	4	10
	3	1	2.5
	SL	21	**52.5**
	5	1	2.5
	6	2	5
	7	2	5
	FP	1	2.5
ΔF-cadherin (n=45)	RP	2	4.5
	1	4	9
	2	4	9
	3	2	4.5
	SL	12	**26.7**
	5	6	13.5
	6	6	13.5
	7	9	20
	FP	0	0
CBR (n=35)	RP	2	6
	1	9	26
	2	3	8.5
	3	4	11
	SL	8	**22.5**
	5	4	11
	6	2	6
	7	1	3
	FP	2	6

Transplants of cells expressing each RNA were made into the prospective alar and basal plate of the neural tube, and analyzed as described in the Materials and Methods. Based on the bin analysis described in Fig. 3, each transplant was placed into a bin that contained the largest percentage of transplanted cells.

*Designation of the bins is described in Fig. 4.

†The number of transplants with a peak location in the indicated bin. One F-cadherin transplant with an equal number of cells in Bins 1 and SL was counted twice.

‡Percentage of transplants with a peak location at the indicated bin.

Table 3. Transplant cell distribution spreads (FWHM analysis)

Injected RNA	Away from sulcus limitans	At sulcus limitans
nlacZ	2.80 (n=25, s.d.=0.764)*	2.57 (n=7, s.d.=1.13)†
F-cadherin	2.75 (n=12, s.d.=1.14)	1.29 (n=7, s.d.=0.488)†,‡
ΔF-cadherin	3.17 (n=12, s.d.=1.40)	1.75 (n=4, s.d.=0.500)‡
CBR	3.33 (n=15, s.d.=1.18)*	3.50 (n=2, s.d.=2.12)

This table presents means of full-width-at-half-maximum (FWHM) values of transplant cell distributions for the various conditions studied. Only dorsal transplants have been considered in this analysis. The numbers in parentheses indicate sample size (n) and standard deviation (s.d.). In each column, the means have been pairwise compared and the superscripts indicate which pairwise differences are significant with $P<0.10$, using one-tailed t-tests; all other pairwise differences are not significant at $P<0.10$. The CBR sample at the sulcus limitans was too small and has not been compared with the other samples. For more details on the FWHM analysis see Materials and Methods. $*P<0.05$. $†P<0.01$. $‡P<0.10$.

limitans. In order to measure the effects of *F-cadherin* expression on cell movements during C-E, we developed an assay based on transplanting marked cells into host embryos, and then following these marked cells during neural tube formation (also see Guthrie et al., 1993). As diagrammed in Fig. 4, small groups of cells from *nLacZ* RNA-injected donor embryos were transplanted into the prospective neural plate of host embryos prior to the onset of C-E. At neural tube stages, when C-E is largely complete, the embryos were fixed, and stained for the expression of *nlacZ* and *F-cadherin*, allowing the distribution of the transplanted cells relative to the sulcus limitans to be determined. As shown in Fig. 4, grafted cells incorporate into the host neural tissue and intercalate during C-E, spreading over considerable distances and mixing extensively with host cells. To measure the extent of these movements, we scored the distribution of transplanted cells in each embryo by dividing the neural tube into a number of radial bins along the D-V axis and scoring the number of cells in each bin (Fig. 4F). We analyzed the overall distribution of the transplanted cells by pooling data from transplants with the same peak location, defined as the bin containing the largest percentage of donor cells, allowing us to generate an average distribution. Plots of these average distributions give one indication of how the transplanted cells distributed within each region of the neural tube during C-E. In addition, the full width at half maximum (FWHM) was analyzed for individual transplant distributions as described in the Materials and Methods.

Bin analysis of *nLacZ*-expressing control cells showed that cell movements during C-E varied in nature depending on the position of the transplanted cells along the D-V axis of the neural tube. In cases where the peak location occurred towards the middle of the alar plate (Fig. 5A), the transplanted cells showed a symmetrical distribution along the D-V axis of the neural tube. A different result was obtained when the peak location of the transplanted cells occurred at the sulcus limitans (Fig. 5B), which is marked by the expression of *F-cadherin*. In these cases, the transplanted cells showed an extremely skewed distribution, with most cells on the alar side and very few on the basal side. We also examined the distribution of cells that were transplanted medially, thus directing them into the basal plate of the host neural tube. As was the case with alar plate transplants, the cells in a transplant with a peak location within the middle of the basal plate were symmetrically distributed along the D-V axis (Fig. 5C), while those with a peak location at the sulcus limitans

in neural or epidermal tissues that were produced when embryos were injected with similar truncated forms of N-cadherin and E-cadherin, respectively (data not shown; Levine et al., 1994). Thus, these results indicate that restricted expression of *F-cadherin* is required for C-E to occur normally. In addition, these results indicate that ΔF-cadherin does not give the same effects as similar truncated forms of E- and N-cadherin, suggesting that it not interfering with the function of other cadherins (Levine et al., 1994).

Transplantation assay

The observations described above suggest a model where the differential expression of *F-cadherin* affects cell movements during neurulation, thus helping to position cells at the sulcus

showed an extremely skewed distribution (Fig. 5D). Thus, these results show that cells disperse within the alar and basal plates during C-E but are restricted from crossing between the alar and basal plates. In addition, cells in both alar and basal plate transplants entered into the stripe of *F-cadherin* expressing cells, indicating that both alar and basal plate cells contribute to the position in the neural tube where *F-cadherin* is expressed.

Computer simulation of cell distributions during neural plate elongation

To examine how the movements of cells during neural plate elongation affect their final distribution along the D-V neuraxis, we developed a computer simulation in which cells move randomly within a tissue but are restricted in their movements at a boundary. In this model, which is described in detail in the Material and Methods, cells are placed on a grid that then elongates via a repeating succession of two steps; a step of random cell rearrangement on the grid and a step of cell movement subject to adhesive forces and opposing diffusion-like processes that tend to spread cells uniformly on the grid. Cells can move up or down and left or right within the interior of the grid, while cells on the left and right borders of the tissue move only to the right or left, respectively, with some bias for moving towards the middle of the D-V axis and outwards in the A-P axis. During each iteration, the grid converges along one axis and extends along the other axis.

When a small group of cells are placed away from the edge of the cell array and disperse during the simulation, their final symmetric distribution mirrors the experimental distribution of transplanted cells whose peak location occurred in the center of the alar or basal plate (compare Fig. 6A with Fig. 5A or C). It is interesting to note that cells spread out as in the experimental case, despite the movement bias mentioned above, which would tend to restrict the spread. In contrast, if a patch of cells is placed closer to the border of the cell array, their subsequent asymmetric distribution mirrors the experimental distribution of cells whose peak location occurs at the sulcus limitans (compare Fig. 6B with Fig. 5B or D). Thus, the experimental measurements of cell dispersion during neurulation are consistent with a model where cells, as they undergo cell rearrangements, move randomly within the alar or basal plates, but encounter a boundary to cell movements at the sulcus limitans.

## Ectopic expression of *F-cadherin* in transplanted cells

The results from the transplantation assay suggest that during C-E, cells disperse along the D-V axis of the neural tube by cell intercalation even though cell movements appear to be restricted across the sulcus limitans, where *F-cadherin* is expressed. This observation suggests several potential roles for F-cadherin in terms of regulating cell movements during C-E. One possibility is that *F-cadherin* expression contributes to the restriction in cell movements between the alar and basal plate. Another possibility is that F-cadherin is not responsible for this boundary, but only for localizing cells at the sulcus limitans. If F-cadherin does indeed localize cells to the sulcus limitans, it might do so on its own by preventing cell dispersion during C-E, or else it might require other factors present at the sulcus limitans in order to influence cell movements. To examine these different possibilities, we asked how the ectopic expression of *F-cadherin* would affect the position of transplanted cells during C-E. Accordingly, donor cells taken from embryos

injected with *F-cadherin* and *nLacZ* RNAs were transplanted into host embryos and subjected to the analysis described above. Control experiments indicated that transplanted cells continued to express exogenous *F-cadherin* protein at high levels out through tadpole stages (data not shown).

Ectopic expression of *F-cadherin* substantially changes the distribution of transplanted cells within the neural tube by several criteria. First, of all the *F-cadherin* transplants analyzed, over half gave a peak location at the sulcus limitans while only a quarter of the control transplants fell into this category (Table 2). Secondly, while control transplants included a number of
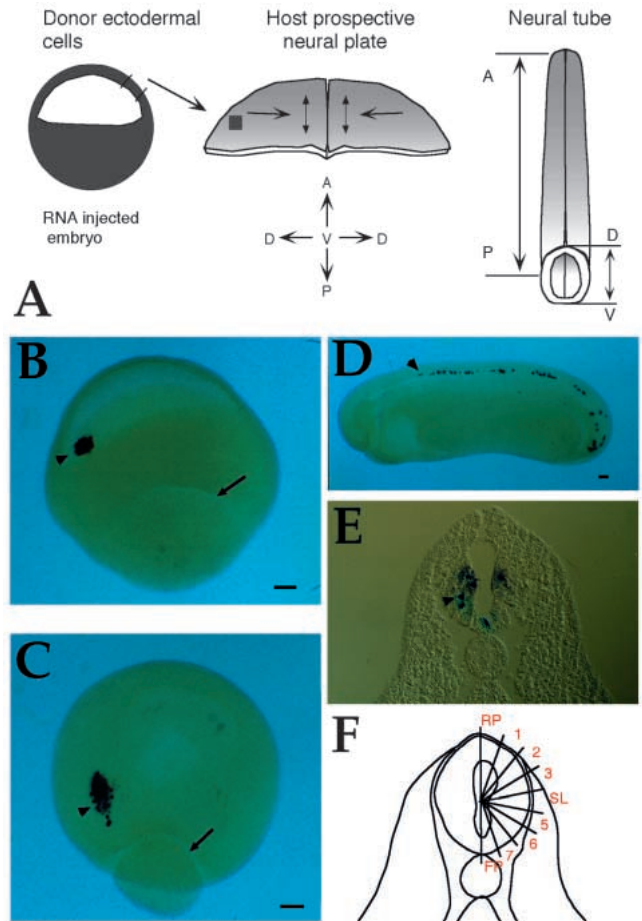
Fig. 4. Bin analysis of cell mixing during convergent-extension. (A) Donor tissue, marked by injection of *nLacZ* RNA was transplanted into the prospective neural plate of host embryos at the beginning of gastrulation. (B-D) Host embryos were stained for β-galactosidase expression to reveal the location of the transplanted cells soon after transplantation (st. 10.5, B), at midgastrulation (st. 11, C), or at neural tube stages (st. 26, D). An arrow points to the dorsal blastopore lip in panels B and C, while transplanted cells are indicated by arrowhead. Note that the transplanted cells incorporate and interact with host cells during convergent-extension. (E,F) Tissue section of a host embryo after staining for β-galactosidase to mark the nuclei of transplanted cells, and whole-mount in situ hybridization for *F-cadherin* expression. In D, the arrowhead points to a transplanted β-galactosidase-expressing cell. In F, the bins used to determine the D-V distribution of transplanted cells are diagrammed. The SL bin was positioned at the site of *F-cadherin* expression. Cells that crossed the roof plate (RP) or floor plate (FP) were assigned to bins designated with a negative sign.
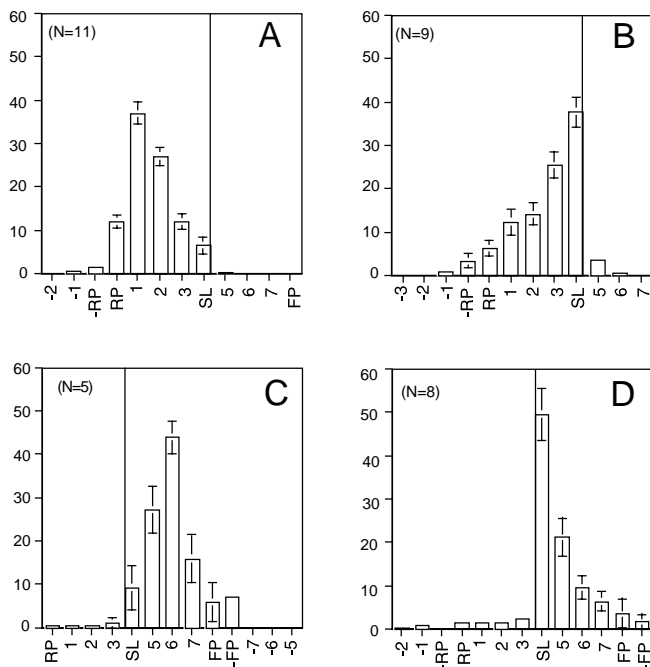
Fig. 5. Average distribution of donor *nLacZ* cells in the posterior neural tube after convergent-extension. (A) Distribution of transplants into the alar plate with a peak location in the bin adjacent to the roof plate (Bin 1). (B) Distribution of transplants into the alar plate with a peak location at the sulcus limitans (Bin SL). (C) Distribution of basal transplants with a peak location at the bin midway between the sulcus limitans and the floor plate (Bin 6). (D) Distribution of basal transplants with a peak location at the sulcus limitans (Bin SL).

examples where the peak location occurred in Bin 3, adjacent to the sulcus limitans, only one of the *F-cadherin* transplants gave this distribution (Table 2). Both of these observations suggest that *F-cadherin*-expressing cells were preferentially localized to the sulcus limitans. Indeed, of the total cells analyzed, 27% of the *F-cadherin*-expressing cells and 13% of the control cells were localized at the sulcus limitans. Thirdly, the distribution of cells in transplants with a peak location at the sulcus limitans showed less of a spread by FWHM analysis than similar transplants of *nLacZ*-expressing cells (Table 3; compare Fig. 7B with Fig. 5B). Finally, when cells expressing *F-cadherin* were transplanted into the middle of the alar plate, their subsequent distribution in the neural tube tended more often to be bimodal, with a second smaller peak occurring at the sulcus limitans (compare Fig. 7A with Fig. 5A). When all transplants into the alar plate are viewed individually, 26% (7/27) of the *F-cadherin*-expressing transplants, but only 5% (2/38) of the *nLacZ*-expressing transplants have bimodal distributions. Thus, all of these observations are strong indications that the differential expression of *F-cadherin* biases cell position to the sulcus limitans during neural tube formation.

F-cadherin appears to be necessary but not sufficient for localizing cells along the D-V axis of the neural tube

The results described above suggest that F-cadherin localizes cells to the sulcus limitans. However these results also suggest that F-cadherin does not mediate this localization by simply limiting the general dispersion of cells during C-E. Thus, in the
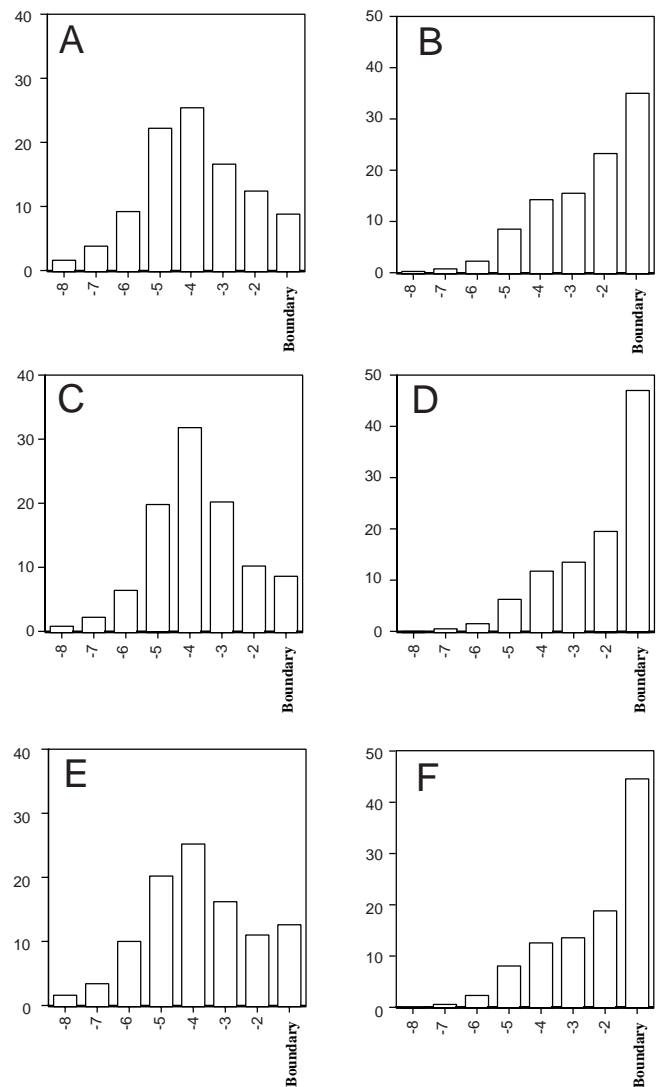
Fig. 6. Results of a computer simulation designed to model the distribution of cells during neural plate elongation. (A,B) Simulation performed with the patch of cells having only default adhesion. (C,D) Simulation performed with the patch of cells adhesive for itself as well as the border of the array. (E,F) Simulation performed with the patch of cells adhesive to the border but not to itself. (A,C,E) Distribution of a patch of cells placed away from the border of the starting array. (B,D,F) Distribution of a patch of cells placed near the border of the starting array.

transplants of *F-cadherin*-expressing cells whose peak location occurred in the middle of the alar plate, the spread of cells along the D-V axis was not statistically different from that of control cells expressing β-galactosidase as determined by FWHM analysis (Table 3; compare Fig. 7A with Fig. 5A). In addition, the A-P distribution of *F-cadherin*-expressing cells did not significantly differ from that of control cells, indicating that F-cadherin does not affect the overall extent of cell movements during C-E (data not shown). Both of these results indicate that F-cadherin does not have a general effect on cell dispersion, or restriction of cell movements during C-E.

To account for how F-cadherin might localize cells during C-E without generally affecting cell dispersion, we examined the

effects of differential cell adhesion on the distributions of cells in our computer simulations. In the first case, we examined a situation where cells in the patch are adhesive both to themselves and to the border of the array. When an 'adhesive' patch of cells is positioned away from the edge of the array, the final distribution of these cells is narrower than that obtained for 'nonadhesive' cells, as expected if adhesion acts to reduce the spread of cells undergoing C-E (Fig. 6C). This outcome is in contrast to that observed experimentally where ectopic expression of F-cadherin does not appear to narrow the final distribution of cells along the D-V axis (Fig. 7A and FWHM analysis in Table 3). We then examined a situation using the model where the cells in the patch are not adhesive to themselves but only to the border of the array. When such cells are started away from the border of the array, they produce bimodal distributions with one peak at the edge of the array. These cells produce a bimodal distribution for start positions that would have led to symmetric distributions had the added adhesion not been there (Fig. 6E). This result mirrored that experimentally observed, i.e. increased incidence of bimodal distributions for *F-cadherin-expressing* transplants with a peak location at the middle of the alar plate (compare Fig. 6E to Fig. 7A). In addition, when a patch of cells, which is adhesive for the border, is started closer to the border of the array, the subsequent distribution is narrower, as also observed experimentally (compare Fig. 6F with Fig. 7C). Thus, the changes in cell position that are observed in *F-cadherin*-expressing, transplanted cells can be explained by a model where F-cadherin affects the adhesion of cells, and thus

cell movements, only when these cells are at the sulcus limitans where F-cadherin is normally expressed.

## ΔF-cadherin prevents cells from localizing precisely at the sulcus limitans

The results obtained above indicate that F-cadherin is one factor required for localizing cells to the sulcus limitans. However, F-cadherin may only contribute substantially to this localization when other factors at the sulcus limitans come into play. To examine this further, we next asked how the inhibition of F-cadherin function might affect cell movements depending on where cells lie along the D-V axis of the neural tube. Accordingly, we transplanted cells expressing Δ*F-cadherin* and determined their distribution using bin analysis (Fig. 8). Significantly, the distribution of cells in transplants expressing Δ*F-cadherin* differed from control cells for those whose peak location occurred at the sulcus limitans. In these cases, cells expressing Δ*F-cadherin* appeared to have crossed the boundary marked by *F-cadherin* expression, and this was true when transplants were made into either the basal or alar plate (Fig. 8). Thus, these results indicate that F-cadherin is necessary for cells to localize at the sulcus limitans during neurulation and that cells disperse from this location when F-cadherin function is inhibited. Importantly, among the transplants of Δ*F-cadherin*-expressing cells, those with peak locations away from the sulcus limitans had a symmetric D-V distribution that was not significantly different from that of control cells by FWHM analysis (Table 3, compare Fig. 8A to Fig. 5A). Therefore, Δ*F-*
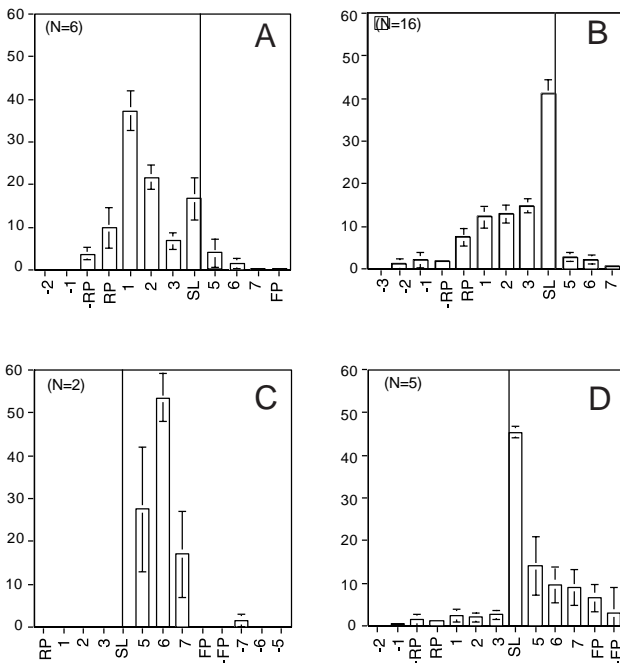
Fig. 7. Average distribution of donor *F-cadherin-expressing* cells in the posterior neural tube after convergent-extension. (A) Distribution for transplants into the alar plate with a peak location in the bin adjacent to the roof plate (Bin 1). (B) Distribution for transplants into the alar plate with a peak location at the sulcus limitans (Bin SL). (C) Distribution of basal transplants with a peak location at the bin midway between the sulcus limitans and the floor plate (Bin 6). (D) Distribution of basal transplants with a peak location at the sulcus limitans (Bin SL).
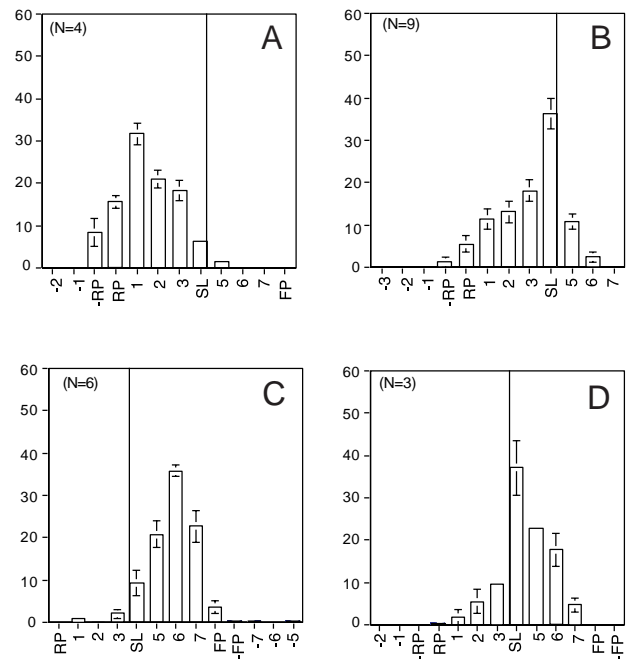
Fig. 8. Average distribution of donor Δ*F-cadherin-MT*-expressing cells in the posterior neural tube after convergent-extension. (A) Distribution for transplants into the alar plate with a peak location in the bin adjacent to the roof plate (Bin 1). (B) Distribution for transplants into the alar plate with a peak location at the sulcus limitans (Bin SL). (C) Distribution of basal transplants with a peak location at the bin midway between the sulcus limitans and the floor plate (Bin 6). (D) Distribution of basal transplants with a peak location at the sulcus limitans (Bin SL).
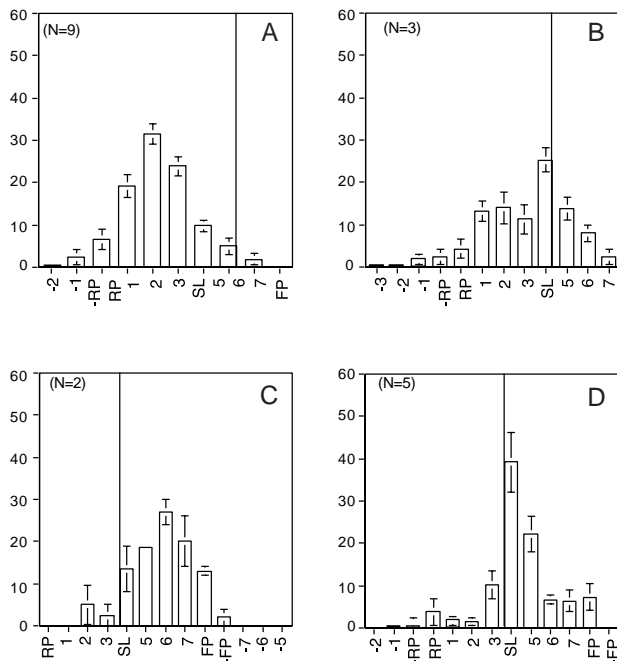
Fig. 9. Average distribution of donor *CBR-MT*-expressing cells in the posterior neural tube after convergent-extension. (A) Distribution of transplants into the alar plate with a peak location in the bin adjacent to the roof plate (Bin 1). (B) Distribution of transplants into the alar plate with a peak location at the sulcus limitans (Bin SL). (C) Distribution of basal transplants with a peak location at the bin midway between the sulcus limitans and the floor plate (Bin 6). (D) Distribution of basal transplants with a peak location at the sulcus limitans (Bin SL).

cadherin affects the movements of cells only at the sulcus limitans where *F-cadherin* is normally expressed.

Inhibition of cadherin function alters position along the D-V axis

The results described above indicate that F-cadherin is likely to be only one factor determining localization of *F-cadherin*-expressing cells to the sulcus limitans. To ask more generally whether cadherin-mediated adhesion contributes to this localization, we examined the effects of generally disrupting cadherin function on the positioning of transplanted cells. We have previously shown that constructs containing just the intracellular domain of N-cadherin are pan-inhibitors of endogenous cadherin function when expressed in *Xenopus* embryos (Kintner, 1992; Riehl et al., 1996). When expressed at high levels, these cytoplasmic constructs cause extensive cell dissociation, but can be titered to a level at which cell dissociation does not occur but adhesion seems to be affected as shown by a general inhibition of C-E (data not shown). Thus, we used one of these cytoplasmic inhibitors, called CBR, to inhibit cadherin-mediated adhesion in transplanted cells during C-E. Cells were taken from embryos injected with *CBR* RNA (5 pg/embryo), transplanted into host embryos and analyzed for their D-V distribution as above. The results show (Fig. 9) that cells expressing *CBR* behave significantly differently from control cells in terms of their distribution along the D-V axis of the neural tube: away from the sulcus limitans, the average spread of CBR transplant distributions in the FWHM analysis
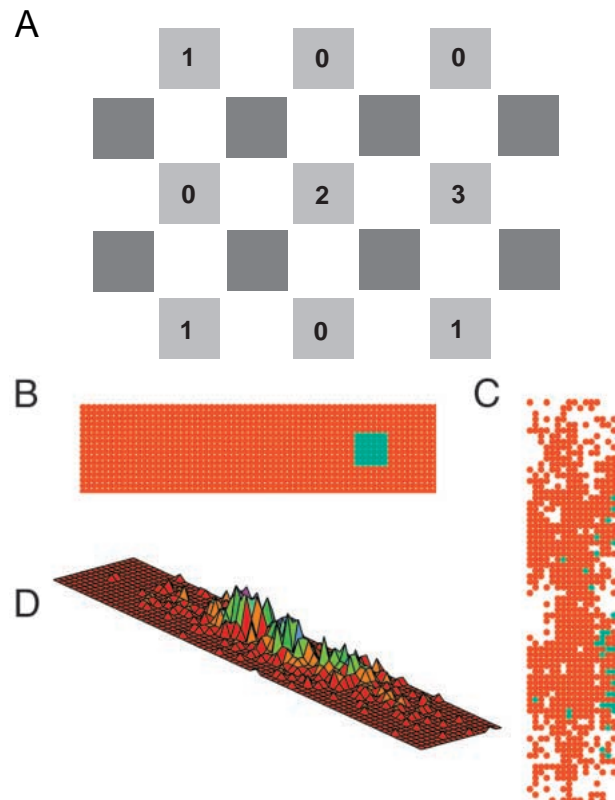
Fig. 10. Computer simulation of cell dispersion during neurulation. (A) The diagram illustrates a rearrangement step of the model, where the dark squares represent the grid of positions of the tissue at the very beginning of the simulation, when each grid position is occupied by a single cell, and the light gray squares represent the tissue after the first rearrangement step when the tissue has shrunk by one column and elongated. The numbers in the light gray squares indicate how many cells have ended up in those grid positions; there are grid positions with no cells and others with more than one cell, the total number of cells on the grid being of course the total number before the rearrangement (8 in this example). Note that cells in the dark squares can move to a grid position either up or down and to the left or right (except for cells at the borders which can move up or down, but to one side only). After this rearrangement step of the algorithm, comes a 'diffusion-adhesion' step which moves cells around on the (light gray) grid (as described in the Methods), then another rearrangement step (from the light gray grid), and so on till the grid has converged and extended to the desired final size. (B-C) Initial and final frames from a simulation run. Patch cells are represented in green. Grid points may contain more than one cell. (D) Final distribution of patch cells on the grid, for a patch that was initially placed towards the middle of the D-V extent of the beginning grid (pooled data from 20 simulations).

is larger than that of controls (Table 3). Also, cells expressing *CBR* tend to cross the sulcus limitans more frequently (Fig. 9B,D), much more than cells expressing Δ*F-cadherin* (Fig. 8B). Thus, while 38% of all CBR transplants (13/34) had more than 10% of the cells which crossed the sulcus limitans, only 22% of all ΔF-cadherin transplants (5/31), and 13% of all control transplants fell into this category (9/70). These results support the idea that cadherin function contributes to the positioning of cells along the D-V neuraxis during C-E, and that *F-cadherin* might be only one of several factors contributing to the localization of cells to the sulcus limitans.

DISCUSSION

During the patterning of the vertebrate CNS, cells acquire a regional identity that reflects their position along the neuraxis. One likely outcome of neural patterning is to endow some cells with the ability to localize within the developing CNS, even during periods of active cell movement such as those occurring during neurulation. The well-established properties of the cadherins are consistent with the idea that differential cell adhesion could be a factor in how cells determine their position within the CNS during neural morphogenesis. For example, in vitro studies have shown that cadherins can promote sorting in cell aggregation assays (Nose et al., 1988; Steinberg and Takeichi, 1994). In addition, dissociated embryonic tissue has been shown to reaggregate in a cadherin specific manner (Matsunami and Takeichi, 1995). The differential expression of cadherins by different tissues in early development and within tissues during regionalization has also suggested a role for cadherins in cell segregation in vivo (Choi and Gumbiner, 1989; Dahl et al., 1996; Ganzler and Redies, 1995; Hatta et al., 1987; Kimura et al., 1995; Kintner, 1992; Nakagawa and Takeichi, 1995; Redies, 1995). Finally, the ectopic expression of *N-cadherin* in *Xenopus* appears to create ectopic boundaries within tissues (Detrick et al., 1990; Fujimori and Takeichi, 1993). These observations have suggested that differential cadherin expression might contribute to the localization of neural cells to different regions, but direct experimental evidence for a such a role has been notably lacking.

F-cadherin expression marks a subdomain in the caudal neural tube.

F-cadherin is expressed by a small population of cells that lie at the boundary between the alar and basal plate (Espeseth et al., 1995). A number of other genes show a pattern of expression that is restricted to this region in the hindbrain and spinal cord, including *XASH-3* in *Xenopus*, *Dbx* in mouse, and the *Dbx* homologs *hlx-1* in zebrafish and *CHoxE* in chick (Fjose et al., 1994; Lu et al., 1992; Rangini et al., 1991; Zimmerman et al., 1993). These observations suggest that the sulcus limitans represents a subdomain of the caudal neural tube, containing cells distinct from other dorsal and ventral cell types. The early expression of *F-cadherin* indicates that this subdomain might form as early as stage 13 when neurulation begins (Espeseth et al., 1995). In addition, the results of the transplantation assay indicate that both dorsal and ventral cells contribute to this subdomain. Thus, we suggest that cells at the sulcus limitans are derived from both the alar and basal plate, perhaps from cells that lie at the boundary between these two domains, and that these cells appear to form a distinct population during neural tube formation, as evident from the stripe of *F-cadherin*-expressing cells at this stage (Fig. 2). Moreover, in this model, the expression of *F-cadherin* by the sulcus limitans cells would presumably allow them to maintain their position in the neural tube during neurulation.

F-cadherin is necessary, but not sufficient, for the localization of cells into a stripe at the sulcus limitans

Using a transplantation assay, we examined the role of F-cadherin in positioning cells at the sulcus limitans during neural tube formation. Our results suggest strongly that differential adhesion is one factor required for cells to localize at the sulcus limitans. When transplanted cells express *F-cadherin,* their localization to the sulcus limitans is markedly increased (Fig. 7). In addition, when F-cadherin function is inhibited in transplanted cells using ΔF-cadherin, cells fail to localize precisely to the sulcus limitans as is evident from the fact that they cross from the basal into alar plate, or vice versa (Fig. 8). Thus, these results suggest strongly that the differential expression of *F-cadherin* is required by cells to localize to the sulcus limitans during the extensive cell movements that occur during neurulation.

Ectopic expression of *F-cadherin* in the surface ectoderm produces a sharp boundary between expressing and nonexpressing *F-cadherin* cells (Fig. 1). Thus we first hypothesized that a similar boundary might form between *F-cadherin*-expressing and nonexpressing cells within the neural tube during neurulation. In this model, the initial broad domain of *F-cadherin* expression observed at the open neural plate stage would give rise to the subsequent narrow stripe of *F-cadherin*-expressing cells in the neural tube, simply because *F-cadherin*-expressing cells tend not to intercalate with non-expressing cells during C-E. This, however, does not appear to be the case. Cells ectopically expressing *F-cadherin* intercalate with non-expressing cells as well as control cells during C-E, as is evident from the spread of transplanted *F-cadherin*-expressing cells along both the D-V and A-P neuraxis (Fig. 7, data not shown). We suggest, therefore, that in terms of regulating cell movements during C-E, the differential expression of F-cadherin is a factor only when cells come in contact with the sulcus limitans where F-cadherin is normally expressed. Indeed, the cell distributions that we observed experimentally can be explained in a computer-simulated model by a case where cells do not have adhesion for themselves (which tends to narrow the final distribution) but instead by one where cells are only adhesive for the edge of the array (i.e. the sulcus limitans). This predicts that the differential expression of *F-cadherin* only influences cell movements at the sulcus limitans where additional factors come into play but is largely irrelevant elsewhere. Among the other factors that could regulate cell position at the sulcus limitans is the restriction in cell movements between the alar and basal plate that can be observed in the transplantation assay. This restriction appears to be co-incident with the *F-cadherin*-expressing cells and a further indication that this region of the neural tube may be specialized in several different ways. A simple model to explain these observations is that several cadherins work together to account for the final distribution of sulcus limitans cells. This model would account for the more dramatic dispersion of cells observed when cadherin function is more generally inhibited with CBR (Fig. 9).

Cell adhesion and neural patterning

We have shown that the differential expression of *F-cadherin* is one factor determining cell position along the D-V axis of the neural tube. This finding may have implications for the processes that pattern the caudal neural tube along its D-V axis. Recent studies suggest that ventral cell types in the neural tube are specified by sonic hedgehog or a related molecule which is secreted from the notochord, while dorsal cell fates appear to be specified by BMP-like molecules, perhaps provided dorsally by the nonneural ectoderm (Ericson et al., 1996; Liem et al., 1995; Tanabe et al., 1995). Moreover these signaling molecules appear to act as morphogens in that they specify different cells

fates along the D-V axis as a function of their concentration (Roelink et al., 1995). If so, then factors such as *F-cadherin* will indirectly affect cell fate by determining the position of cells relative to the source of the dorsal and ventral morphogens. Thus, neural patterning may involve an interplay between the signals that initially specify cell fate according to position within the neural tube, and factors such as F-cadherin which determine position by mediating differential adhesion.

REFERENCES

Chitnis, A., Henrique, D., Lewis, J., Ish-Horowicz, D. and Kintner, C. (1995). Primary neurogenesis in *Xenopus* embryos regulated by a homologue of the Drosophila neurogenic gene Delta. *Nature* **375**, 761-766.

Choi, Y.-S. and Gumbiner, B. (1989). Expression of cell adhesion molecule E-cadherin in *Xenopus* embryos begins at gastrulation and predominates in the ectoderm. *J. Cell Biol.* **108**, 2449-2458.

Coffman, C. R., Skoglund, P., Harris, W. A. and Kintner, C. R. (1993). Expression of an extracellular deletion of Xotch diverts cell fate in *Xenopus* embryos. *Cell* **73**, 659-671.

Dahl, U., Sjodin, A. and Semb, H. (1996). Cadherins regulate aggregation of pancreatic beta-cells in vivo. *Development* **122**, 2895-2902.

Detrick, R. J., Dickey, D. and Kintner, C. R. (1990). The effects of N-cadherin misexpression on morphogenesis in *Xenopus* embryos. *Neuron* **4**, 493-506.

Ericson, J., Morton, S., Kawakami, A., Roelink, H. and Jessell, T. M. (1996). Two critical periods of Sonic Hedgehog signaling required for the specification of motor neuron identity. *Cell* **87**, 661-673.

Espeseth, A., Johnson, E. and Kintner, C. (1995). *Xenopus* F-cadherin, a novel member of the cadherin family of cell adhesion molecules, is expressed at boundaries in the neural tube. *Mol. Cell. Neurosci.* **6**, 199-211.

Evan, G. I., Lewis, G. K., Ramsay, G. and Bishop, J. M. (1985). Isolation of monoclonal antibodies specific for human c-myc proto-oncogene product. *Mol. Cell Biol.* **5**, 3610-3616.

Fjose, A., Izpisua-Belmonte, J. C., Fromental-Ramain, C. and Duboule, D. (1994). Expression of the zebrafish gene *hlx-1* in the prechordal plate and during CNS development. *Development* **120**, 71-81.

Fujimori, T. and Takeichi, M. (1993). Disruption of epithelial cell-cell adhesion by exogenous expression of a mutated nonfunctional N-cadherin. *Mol. Biol. Cell* **4**, 37-47.

Ganzler, S. I. and Redies, C. (1995). R-cadherin expression during nucleus formation in chicken forebrain neuromeres. *J. Neurosci.* **15**, 4157-4172.

Geiger, B. and Ayalon, O. (1992). Cadherins. *Annu. Rev. Cell Biol.* **8**, 307-332.

Guthrie, S., Prince, V., and Lumsden, A. (1993). Selective dispersal of avian rhombomere cells in orthotopic and heterotopic grafts. *Development* **118**, 527-538.

Harland, R. M. (1991). In situ hybridization: an improved whole-mount method for *Xenopus* embryos. *Methods Cell Biol.* **36**, 685-695.

Hatta, K., Takagi, S., Fujisawa, J. and Takeichi, M. (1987). Spatial and temporal expression pattern of N-cadherin cell adhesion molecules correlated with morphogenetic processes of chicken embryos. *Dev. Biol.* **120**, 215-227.

Hynes, R. O. (1996). Targeted mutations in cell adhesion genes: what have we learned from them? *Dev. Biol.* **180**, 402-412.

Keller, R., Shih, J. and Sater, A. (1992). The cellular basis of the convergence and extension of the *Xenopus* neural plate. *Dev. Dyn.* **193**, 199-217.

Kimura, Y., Matsunami, H., Inoue, T., Shimamura, K., Uchida, N., Ueno, T., Miyazaki, T. and Takeichi, M. (1995). Cadherin-11 expressed in association with mesenchymal morphogenesis in the head, somite, and limb bud of early mouse embryos. *Dev. Biol.* **169**, 347-358.

Kintner, C. (1988). Effects of altered expression of the neural cell adhesion molecule, N-CAM, on early neural development in *Xenopus* embryos. *Neuron* **1**, 545-555.

Kintner, C. (1992). Regulation of embryonic cell adhesion by the cadherin cytoplasmic domain. *Cell* **69**, 225-236.

Kuhl, M., Finnemann, S., Binder, O. and Wedlich, D. (1996). Dominant negative expression of a cytoplasmically deleted mutant of XB/U-cadherin disturbs mesoderm migration during gastrulation in *Xenopus laevis. Mech. Dev.* **54**, 71-82.

Lee, C. H. and Gumbiner, B. M. (1995). Disruption of gastrulation movements in *Xenopus* by a dominant-negative mutant for C-cadherin. *Dev. Biol.* **171**, 363-373.

Levine, E., Lee, C. H., Kintner, C. and Gumbiner, B. M. (1994). Selective disruption of E-cadherin function in early *Xenopus* embryos by a dominant negative mutant. *Development* **120**, 901-909.

Liem, K. J., Tremml, G., Roelink, H. and Jessell, T. M. (1995). Dorsal differentiation of neural plate cells induced by BMP-mediated signals from epidermal ectoderm. *Cell* **82**, 969-979.

Lu, S., Bogard, L. D., Murtha, M. T. and Ruddle, F. H. (1992). Expression pattern of a murine homeobox gene, Dbx, displays extreme spatial restriction in embryonic forebrain and spinal cord. *Proc. Natl. Acad. Sci. USA* **89**, 8053-8057.

Matsunami, H. and Takeichi, M. (1995). Fetal brain subdivisions defined by R- and E-cadherin expressions: evidence for the role of cadherin activity in region-specific, cell-cell adhesion. *Dev. Biol.* **172**, 466-478.

Nakagawa, S. and Takeichi, M. (1995). Neural crest cell-cell adhesion controlled by sequential and subpopulation-specific expression of novel cadherins. *Development* **121**, 1321-1332.

Nose, A., Nagafuchi, A. and Takeichi, M. (1988). Expressed recombinant cadherins mediate cell sorting in model systems. *Cell* **54**, 993-1001.

Ozawa, M., Baribault, H. and Kemler, R. (1989). The cytoplasmic domain of the cell adhesion molecule uvomorulin associates with three independent proteins structurally related in different species. *EMBO J.* **8**, 1711-1717.

Rangini, Z., Ben-Yehuda, A., Shapira, E., Gruenbaum, Y. and Fainsod, A. (1991). CHoxE, a chicken homeogene of the H2. O type exhibits dorso-ventral restriction in the proliferating region of the spinal cord. *Mech. Dev.* **35**, 13-24.

Redies, C. (1995). Cadherin expression in the developing vertebrate CNS: from neuromeres to brain nuclei and neural circuits. *Exp. Cell Res.* **220**, 243-256.

Redies, C., Engelhart, K. and Takeichi, M. (1993). Differential expression of N- and R-cadherin in functional neuronal systems and other structures of the developing chicken brain. *J. Comp. Neurol.* **333**, 398-416.

Redies, C. and Takeichi, M. (1993). Expression of N-cadherin mRNA during development of the mouse brain. *Dev. Dyn.* **197**, 26-39.

Redies, C. and Takeichi, M. (1996). Cadherins in the developing central nervous system: an adhesive code for segmental and functional subdivisions. *Dev. Biol.* **180**, 413-423.

Riehl, R., Johnson, K., Bradley, R., Grunwald, G. B., Cornel, E., Lilienbaum, A. and Holt, C. E. (1996). Cadherin function is required for axon outgrowth in retinal ganglion cells in vivo. *Neuron* **17**, 837-848.

Roelink, H., Porter, J. A., Chiang, C., Tanabe, Y., Chang, D. T., Beachy, P. A. and Jessell, T. M. (1995). Floor plate and motor neuron induction by different concentrations of the amino-terminal cleavage product of sonic hedgehog autoproteolysis. *Cell* **81**, 445-455.

Sano, K., Tanihara, H., Heimark, R. L., Obata, S., Davidson, M., St John, T., Taketani, S. and Suzuki, S. (1993). Protocadherins: a large family of cadherin-related molecules in central nervous system. *EMBO J.* **12**, 2249-2256.

Shimamura, K. and Takeichi, M. (1992). Local and transient expression of E-cadherin involved in mouse embryonic brain morphogenesis. *Development* **116**, 1011-1019

Steinberg, M. S. and Takeichi, M. (1994). Experimental specification of cell sorting, tissue spreading, and specific spatial patterning by quantitative differences in cadherin expression. *Proc. Natl. Acad. Sci. USA* **91**, 206-209

Suzuki, S., Sano, K. and Tanihara, H. (1991). Diversity of the cadherin family: evidence for eight new cadherins in nervous tissue. *Cell Reg.* **2**, 261-270.

Takeichi, M. (1991). Cadherin cell adhesion receptors as a morphogenetic regulator. *Science* **251**, 1451-1455.

Takeichi, M. (1995). Morphogenetic roles of classic cadherins. *Curr. Opin. Cell Biol.* **7**, 619-627.

Tanabe, Y., Roelink, H. and Jessell, T. M. (1995). Induction of motor neurons by Sonic hedgehog is independent of floor plate differentiation. *Curr. Biol.* **5**, 651-658.

Turner, D. and Weintraub, H. (1994). Expression of achaete-scute homolog 3 in *Xenopus* embryos converts ectodermal cells to a neural fate. *Genes Dev.* **8**, 1434-1447.

Zimmerman, K., Shih, J., Bars, J., Collazo, A. and Anderson, D. J. (1993). XASH-3, a novel *Xenopus* achaete-scute homolog, provides an early marker of planar neural induction and position along the mediolateral axis of the neural plate. *Development* **119**, 221-232.